A chemical coating strategy for assembling a boron-doped diamond anode towards electrocatalytic degradation of late landfill leachate†

Juanmei Zeng,[a] Xi Liu,[b] Qizhi Chen[c] and Dongying Hu [ID] *[a]

The high efficiency electrocatalytic degradation of late landfill leachate is still not an easy task due to the complexity and variability of organic pollutants. A chemical coating strategy for assembling a boron-doped diamond anode (BDD) towards electrocatalytic degradation of late landfill leachate was adopted and studied. The results shows the high removal rates of organic carbon (TOC) and ammonia nitrogen (NH_3-N) after electrochemical oxidation for 5 h can reach 99% and 100%. Further, the organic migration and transformation depends on current density, A/V value, initial pH, electrochemical degradation time, and composition of the stock solution. Specifically, alkaline conditions can increase both TOC and NH_3- N removal rates, which is reflected in the NH_3-N removal rate of 100% when the pH is 8.5 after only 5 h. The types of organic matter decreased from 63 species to 24 species in 5 h, in which the removal of fulvic acids is superior to that of soluble biometabolites. Amides/olefins and phenolic alcohols are all degraded and converted into other substances or decomposed into CO_2 and H_2O by BDD, accompanied by the continuous decomposition of alcohol-phenols into alkanes. In all, this study provides a core reference on electrocatalytic degradation of late landfill leachate.

1 Introduction

Late landfill leachate is a kind of high concentration organic wastewater with high pollution intensity and complex components, and its direct discharge without treatment will cause serious secondary pollution to the water environment.[1,2] The late landfill leachate has the characteristics of serious imbalance of nutrient elements, high concentration of ammonia nitrogen and poor biodegradability.[3] Due to the poor pollutant removal effect of traditional biological treatment, the combined process of "physical/chemical treatment" and "biological treatment" is more suitable for deep treatment of late landfill leachate.[4] As a powerful advanced oxidation technology, the electrochemical oxidation method has the advantages of versatility, simple operation, no or few chemicals, easy automatic management, no secondary pollution and so on.[5] In recent years, it has received extensive attention in the field of refractory wastewater, especially for late landfill leachate.[6]

The development of high-performance electrodes with high activity and long service life plays a decisive role applying for various fields.[7–9] Particularly in biodegradable wastewater,[10] various anodes including Fe/C granules,[11] Ti-based mixed metal oxide (MMO) anodes (RuO_2-TiO_2, RuO_2-IrO_2, PtO_2-IrO_2, and $IrO_2-Ta_2O_5$).[12,13] $Fe_3O_4/N-rGO$,[14] and membrane-based electrode engineering[15] and boron-doped diamond (BDD)[16] were also developed and applied to the electrochemical oxidation of late landfill leachate. In contrast, the effect of Fe_3O_4-RGO electrode to improve the biodegradability of leachate depends on high current density, resulting in low COD removal rate of 64.7%.[17] The COD removal efficiency by Fe-NiCAF/O_3 only increased from 39% to 57% compared with ozonation for high-concentration landfill leachate.[18] Ti–Ru–Sn ternary oxide ($TiRuSnO_2$) anode achieved a COD removal rate of 35%.[19] BDD electrode has excellent electrochemical properties, especially wide electrochemical potential window, low background current, good corrosion resistance, high stability, and long service life.[20] It was mainly used as electrode on electrochemical oxidation of organic matter, involving carcinoembryonic antigen and carcinoma antigen,[21] phenols and aniline organics,[22] azo dye Orange G,[23] *Escherichia coli*-contaminated water,[24] X-GN dye wastewater,[25] *et al.* BDD electrode modified by bimetallic NiCu catalysts show a 44.8% of NH_3-N oxidation

[a]State Key Laboratory of Featured Metal Materials and Life-cycle Safety for Composite Structures, School of Resources, Environment and Materials, Guangxi University, Nanning 530004, China. E-mail: hdy@gxu.edu.cn; 1184604205@qq.com

[b]Guangxi Environmental Protection Industry Development Research Institute Co., Ltd, Guangxi Key Laboratory of Environmental Pollution Control and Ecological Restoration Technology, Nanning 530007, China. E-mail: liuxi1217@foxmail.com

[c]Guangxi Huiyuan Manganese Industry Co., Ltd, Laibin 546100, China. E-mail: 184170581@qq.com

† Electronic supplementary information (ESI) available. See DOI: https://doi.org/10.1039/d4ra03107e

efficiency in 6 h.[26] The electrochemical degradation showed that chemical oxygen demand (COD) was decreased from 67.8%, 69.0% and 71.8% on BDD, and 76.4%, 84.3% and 91.9% on Pt NPs/BDD with current densities increased from 15, 50 to 100 mA cm^{-2}.[27] Specifically, BDD electrode showed efficient removal rates for COD (87.5%) and NH$_3$–N (74.06%) after 6 h in the treatment of late landfill leachate.[28] However, the water quality characteristics and electrochemical degradation conditions (current densities, anode area/solution volume (A/V) values, pH values, chloride area concentration, electrolysis time) of late landfill leachate differ in improving the biodegradability of landfill leachate.[29] Systematic research on electrochemical oxidation process is particularly important and urgent for the further treatment of landfill leachate.

More importantly, active chlorine is involved in the oxidation of both organic matter and NH$_3$–N, and there is competition between the removal of COD and NH$_3$–N, involving a complex reaction mechanism of the electrochemical oxidation of landfill leachate.[30] In addition, the competition between direct oxidation reaction and indirect oxidation reaction for the corresponding relationship between COD and NH$_3$–N removal effect is still to be improved.[31] So, there is still a lack of an in-depth and systematic research for the mechanism of organic migration and transformation of late landfill leachate by electrocatalytic degradation on BDD anode to the best of our knowledge.[32] In view of the complexity of organic compounds in leachate treated effluent, it is important to explore the reaction mechanism of organic compounds removal by electrochemical oxidation from the perspective of molecular structure and species.[33] Further research on the migration and transformation of ammonia nitrogen in the electrochemical oxidation process can provide solutions for the effective removal of ammonia nitrogen.[34] So, the high efficiency electrocatalytic degradation of late landfill leachate and its mechanism of organic migration and transformation are still not an easy task due to the complexity and variability of organic pollutants.

Herein, the boron-doped diamond (BDD) was deposited on a Si substrate via hot-filament chemical vapor deposition (HFCVD) for electrochemical oxidation of late landfill leachate (Fig. 1). On one side, the morphologies and growth characteristics of boron-doped diamond on Si substrate were displayed and analyzed by XRD, Raman, SEM, and EDS mapping. Following, the electrochemical properties of BDD electrode were tested and analyzed through CV, EIS, and LSV curves. On the other side, the effects of current density, initial pH, A/V value and electrolysis time on the removal of organic pollutants and ammonia nitrogen during electrochemical oxidation of late landfill leachate were studied. Far beyond that, mechanism of organic migration and transformation of late landfill leachate by BDD anode has been systematically studied, relying on three-dimensional fluorescence spectroscopy (EEM) and Gas chromatography-mass spectrometry (GC-MS). Apart from the above analysis, the relationship between pH change, temperature of landfill leachate at initial and final situation are further invested for the analysis of the mechanism of electrochemical oxidation. Overall, this study provides the core reference for the development of short-range, high efficiency and easy operation of leachate advanced treatment technology. List of abbreviations is shown in Table S1.†

2 Materials and methods

2.1 Deposition of a boron-doped diamond thin film on a Si substrate

All chemicals were used without purification treatment and purchased from Aladdin Co., Ltd, China. The boron-doped diamond (BDD) is deposited on a Si substrate via hot-filament chemical vapor deposition (HFCVD) by referring to previous work.[35] First, a silicon wafer (p type, 100 crystal direction, Huake Electronic Materials Co., Ltd, Zhejiang, China) is polished to remove surface oxides and other contaminants, and then ultrasonic cleaned in ultra-pure water and ethanol for 15 min. The treated Si substrate is then transferred to a mixed solution with diamond powder of 1 mg mL^{-1} (average particle size ≈ 50 nm), and the nucleation site is formed by ultrasound for 75 min. The following deposition process is conducted in a mixture of methane (CH$_4$), hydrogen (H$_2$), and boron sources under a pressure of 5 kPa. The liquid trimethyl borate (B(OCH$_3$)$_3$) as boron source is introduced into the CVD chamber by bubbling hydrogen (H$_2$) gas. In the deposition process, the flow rates of CH$_4$, H$_2$ and boron sources are 6, 300 and 336 sccm, respectively. A DC bias electric field is applied between the sample station and the filament holder to gradually adjust the bias current and voltage to 10 A and 200 V. BDD/Si electrodes can be obtained by adjusting the distance between Si substrate and filament to 3 cm, substrate temperature to 950 °C and deposition time to 8 h. The detailed schematic illustration is depicted in Fig. 1a.

2.2 Characterization of boron-doped diamond anode

The X-ray diffraction (XRD) patterns of boron-doped diamond anode and Si substrate were recorded by an X-ray diffractometer (D_{max}-2500VBX, Rigaku, Japan). The Raman spectra of boron-doped diamond anode and Si substrate were performed by a Raman spectrometer (inVia Reflex, Renishaw, UK). The cross-section and longitudinal-section morphologies of boron-doped diamond anode and Si substrate were obtained by a field-emission scanning electron microscope (Nova nano SEM 230, FEI, Netherlands) equipped with an energy-dispersive X-ray (EDS) spectrometer. The landfill leachate after electrochemical oxidation was diluted 150 times with distilled water, and the three-dimensional fluorescence spectrum (EEM) of the samples was determined by fluorescence spectrometer (Hitachi F-4500, Hitachi, Japan). Specifically, the scanning conditions are as follows: EX/EM scanning range is 200–500 nm/220–650 nm, interval is 5 nm, scanning rate is 60 000 nm min^{-1}; PMT voltage is 550 V, response time is 0.002 s. The intermediates formed during electrocatalytic degradation were analyzed by gas chromatography-mass spectrometry (GC-MS) (7890A-G7038A QZLYY003, Tsushima, Japan). The specific test conditions were as follows: the chromatographic column is Hp-5 ms quartz capillary tube (30 m × 0.25 mm × 0.25 μm), the carrier gas is high purity helium with the flow rate of 1.0 mL min^{-1}, the linear
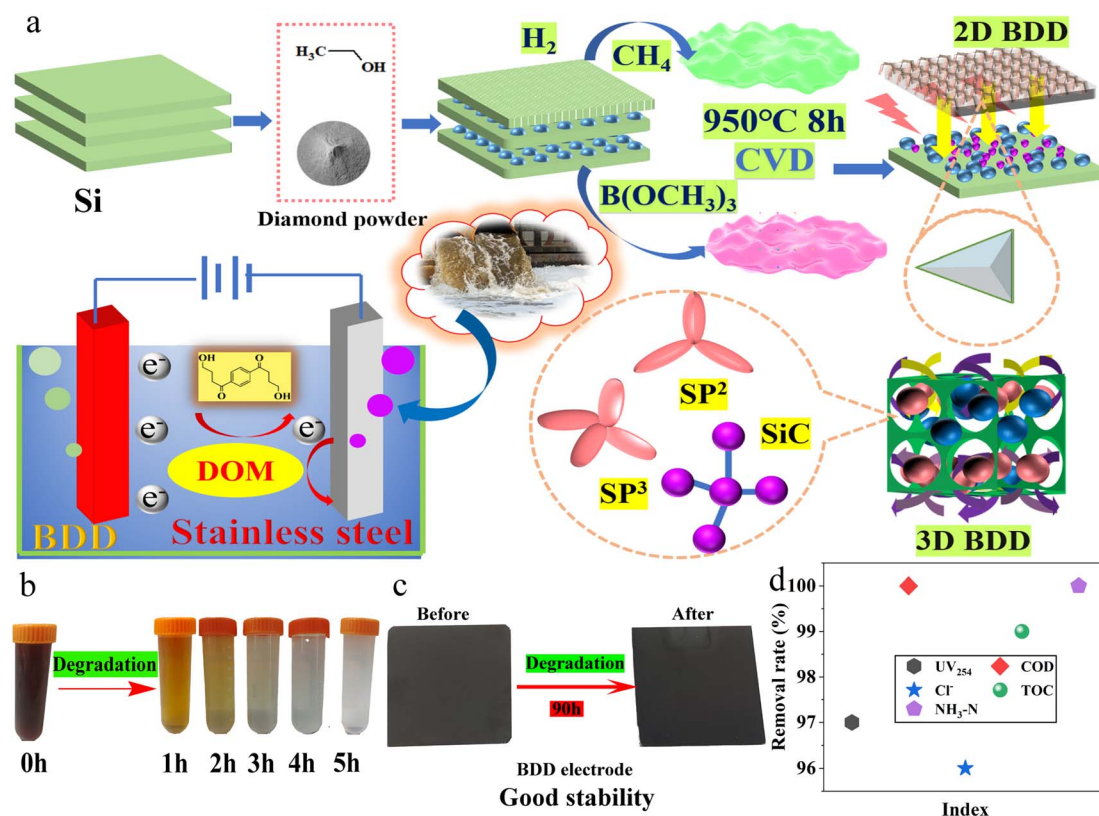
Fig. 1 Scheme of the fabrication of boron-doped diamond anode (a) for electrocatalytic degradation of late landfill leachate (b and c) with efficient purification effect (d).

velocity of 36 cm s^{-1}, and the column pressure at 7.7 Psi. Further, the heating procedure consisted of holding the column temperature at 50 °C for 3 min and rising to 280 °C at 8 °C min^{-1}. Mass spectrum ion source was used with the ion source temperature at 230 °C, the four-pole temperature at 150 °C, the transmission line temperature at 240 °C, and the EM gain factor was 1 with the EM voltage of 1196 V, and the scanning ranging from 40 to 500 amu. The energy consumption of the system was determined by the following eqn (1).[36]

$$E = U \times I \times t/V \times (\Delta COD)_t \qquad (1)$$

I stand for the applied current (A), t is the electrolysis time (h), U is the voltage (V), V is the solution volume (L) and $(\Delta COD)_t$ is the experimental COD concentration decay (mg L^{-1}).

The electrochemical performance of BDD electrode was tested by electrochemical workstation (Xinfeng Technology Co., Ltd, China) with BDD (17 cm^2) as working electrode, platinum sheet as opposing electrode, and Ag/AgCl (sat. KCl) as reference electrode in a three-electrode test system. Specifically, cyclic voltammetry (CV) and Nyquist (EIS) curves were recorded in a 4 mM K$_3$[Fe (CN)$_6$] + 1 M KCl solution at different scan rates of 10–50 mV s^{-1} in the frequency range of 0.01–100 kHz. The polarization curves of BDD electrodes at 50 mV s^{-1} were recorded with and without 50 mg L^{-1} landfill leachate in 0.5 M H$_2$SO$_4$ or 0.1 M Na$_2$SO$_4$ solution. The potential of these BDD electrodes for landfill leachate was measured on a 3 V current

density–time curve by electrocatalytic oxidation. The concentration of hydroxyl radical was detected by the trapping ability of N-subunit *N*-methylaniline.

2.3 Electrocatalytic degradation of late landfill leachate

Late landfill leachate was obtained from BOSSCO Environmental Technology Co., Ltd, China. The composition of the late landfill leachate is 8 of pH at 20 °C, 2523 mg L^{-1} of COD (chemical oxygen demand), 150 mg L^{-1} of BOD$_5$ (5 days biochemical oxygen demand), 1721 mg L^{-1} of TOC (total organic carbon), 1249.5 mg L^{-1} of chloride, 9.85 mg L^{-1} of UV$_{254}$, 39.71 mg L^{-1} of NH$_3$–N (ammonia nitrogen), 115.8 mg L^{-1} of NO$_3$–N (nitrate), 267.25 mg L^{-1} of TN (total nitrogen), 16.4 mS cm^{-1} of electrical conductivity.

The late landfill leachate was degraded by electrocatalysis in a batch electrochemical reactor. BDD and stainless steel were used as the anode and cathode with the adopted effective area (17 cm^2) and a fixed distance of 5 cm. The effects of different current densities (50 mA cm^{-2}, 70 mA cm^{-2}, 90 mA cm^{-2}), different A/V values (3.4 m^{-1}, 4.25 m^{-1}, 5.67 m^{-1}), and initial pH values (5.5, 7, 8.5) on the degradation performance were tested and collected to study the degradation mechanism. Concretely, conductivity was measured using a conductivity meter (DDS-11A). The pH was measured by pH meter (E-201). The concentration of UV$_{254}$, COD, NH$_3$–N, TOC, BOD$_5$, NO$_3$–N, TN, and chloride were measured by UV–Vis absorption (254

nm), potassium dichromate titration (reflux digestion), Nessler's reagent colorimetry, total organic carbon analyzer, dilution inoculation method, UV–Vis absorption (275, 220 nm), alkaline potassium persulfate ultraviolet spectrophotometry, and silver nitrate titration, respectively.

3 Results and discussion

BDD electrode with the best overall performance: the electrocatalytic degradation of late landfill leachate to reach 100% removal rate of COD, 99% removal rate of TOC, 97% of UV_{254}, 100% of NH_3–N, 180.9 mg L^{-1} content of NO_3–N, Cl^- removal of 96%, pH of 7.6, has been fabricated using Si wafer as substrate *via* a simple hot-filament chemical vapor deposition (HFCVD) in Fig. 1b–d. As a result, the morphologies of obtained BDD were displayed in Fig. 2a and b. As shown in Fig. S1,† after 90 h of degradation, the electrode surface remains intact and it still retains good electrochemical degradation properties (Fig. S2†), indicating its good stability.

Compared with the surface morphology of Si substrate, the diamond grains on the surface of BDD electrode are mainly exposed with triangular (111) crystal faces.[37] In addition, a small amount of pore structure and uneven surface morphology are conducive to increasing the contact surface between BDD electrode and late landfill leachate, and improving the electrochemical degradation efficiency. Further, the typical uniform V-shaped structure of diamond was observed on the Si substrate, which further confirmed the successful fabrication of BDD electrode in Fig. 2b.[38] Apparently, the uniform distribution of C and B elements on the surface of the BDD electrode, coupled with up to 96% of C content, indicates that diamond are well doped with boron on the Si substrate in Fig. 2c and d.

In order to further explore the growth characteristics of boron-doped diamond, XRD patterns of BDD electrode and Si matrix were analyzed (Fig. 2e).[39] The diffraction patterns of BDD are located at 43.9° and 75.3°, corresponding to the (111) and (220) crystal faces of the diamond, respectively. In addition to the diamond phase, the (400) diffraction plane (corresponding to $2\theta = 69.1°$) can also be observed with a reduced peak strength, indicating a good combination of Si and diamond. Besides, no corresponding carbide characteristic pattern was observed on BDD electrode, which is related to the fast nucleation rate of diamond on Si substrate and the low SiC content.[40] The characteristic absorption peaks at 1324 cm^{-1} and 285 cm^{-1} attributed to diamond and B were also confirmed by Raman spectra in Fig. 2f. Moreover, the asymmetry of diamond peaks is caused by the Fano effect caused by doped boron atoms.[41] Indeed, the boron-doped diamond electrode on silicon substrate was successfully conducted and expected to contribute excellent electrochemical degradation ability of late landfill leachate.
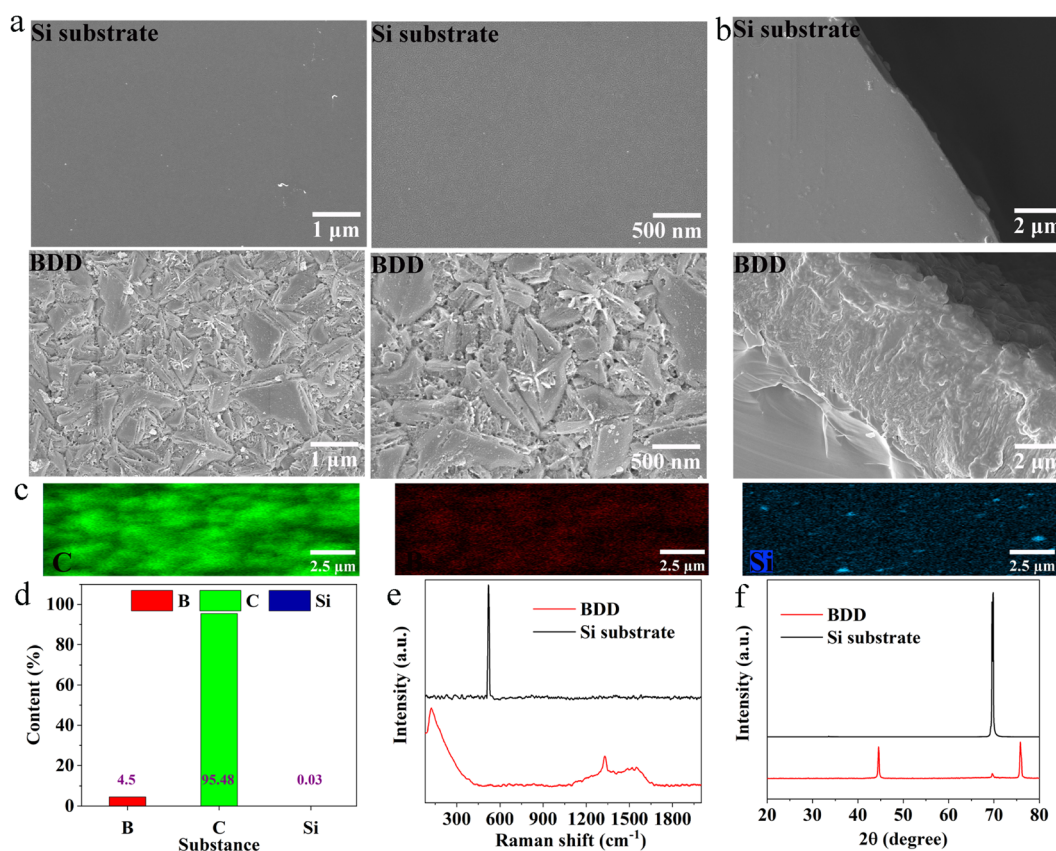

Fig. 2 The morphology of surface (a) and cross-section (b) and EDS scanning of C, B elements (c and d), XRD patterns (e) and Raman patterns (f) of BDD electrode and Si substrate.

Paper

Before assembling electrochemical degradation ability of late landfill leachate, the electrochemical properties of BDD electrode were tested and analyzed through CV, EIS, and LSV curves in Fig. 3. Correspondingly, the CV curves of BDD electrode were evaluated in $K_3[Fe(CN)_6]$ solution (Fig. 3a). Clearly, BDD electrode showed two clearly symmetrical oxidation-reduction peaks. The linear relationship between the peak anode/cathode current and the RMS of the scanning rate confirms that a reversible electrochemical reaction controlled by mass diffusion occurs at the BDD electrode, with a maximum difference of 1.08 mA cm^{-2} between the oxidation and reduction peaks (Fig. 3b). Nevertheless, the reversibility of the electron pairs is further supported by the Randles–Sevcik equation.

Nyquist curves for EIS and Randles equivalent circuit tests are shown in Fig. 3c. The Nyquist curve consists of an arc in the middle and high frequency region and a slash in the low frequency region. The Randles equivalent circuit includes the internal resistance (R_s) of the electrochemical system, the charge transfer resistance (R_{ct}) at the electrode/solution interface, the Warburg impedance (Z_w) of material diffusion, and the constant phase element (CPE) of the double-layer capacitor.[42,43] R_{ct} reflects the electron transfer ability of the electrode at the liquid–solid interface and is an important parameter to characterize the electrode performance. The R_s and R_{ct} values of BDD electrode are 1.54 Ω and 11.75 Ω, indicating a fast ion transport, which is beneficial for increasing the degradation rate. The BDD electrode has an extremely low specific surface area of 9.42 m^2 g^{-1}, which contribute to reduce side reactions, consequently increasing the degradation rate.

In addition, the Oxygen evolution potential (OEP) of BDD electrode was measured by LSV curve in Fig. 3e–h. A higher OEP means that less oxygen is likely to be produced, and the production of more hydroxyl radicals ($\rightsquigarrow$OH) facilitates the oxidation of organic compounds on the electrode surface. As can be seen from Fig. 3e and f, the OEP of BDD electrode at 0.1 M Na_2SO_4 and 0.5 M H_2SO_4 is 1.66 V and 2.41 V, respectively, and the OPE of BDD electrode at the addition of 50 mg L^{-1} landfill leachate is 1.27 V, indicating that the presence of species that start to be oxidized at lower potentials. To further investigate the electrocatalytic degradation capacity of the BDD electrode, current density–time curves were recorded in 0.1 M Na_2SO_4 with and without 50 mg L^{-1} landfill leachate (Fig. 3d). When no landfill leachate was added, the response current density of BDD electrode was 14.06 mA cm^{-2}, and when landfill
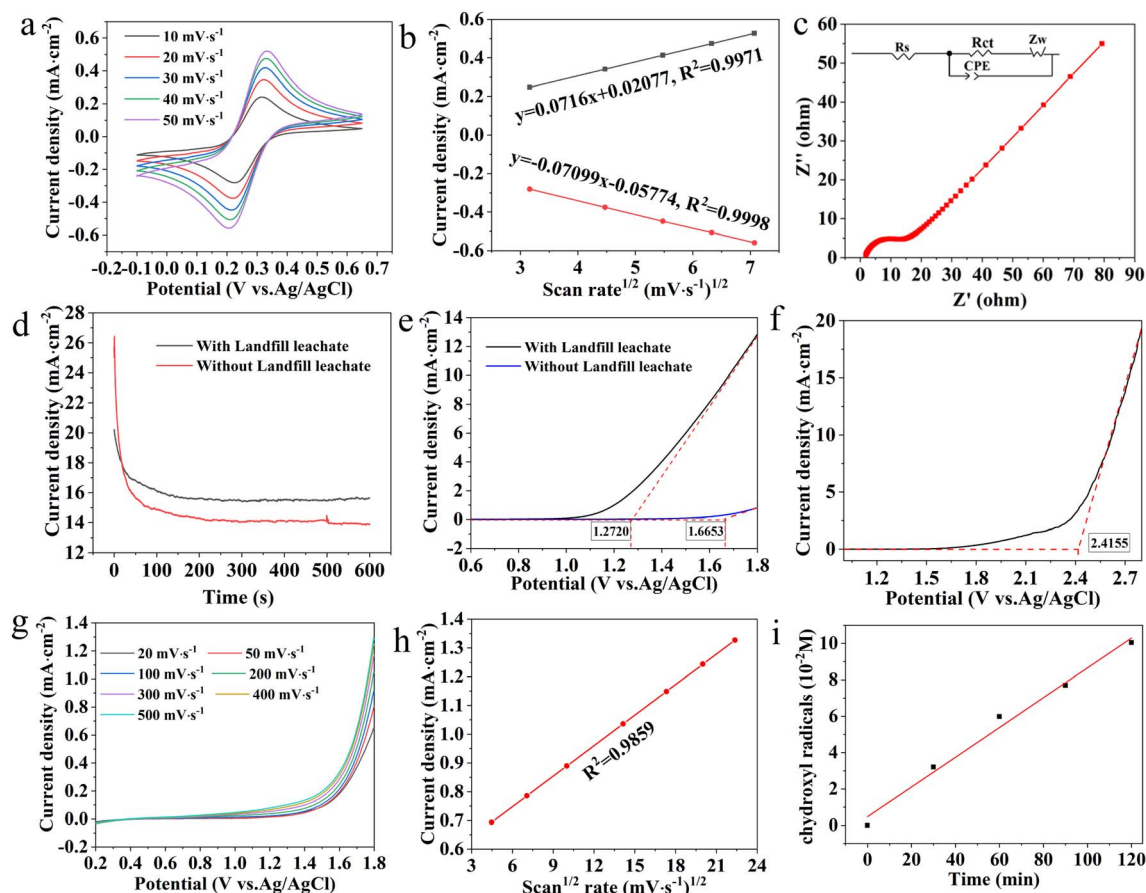

Fig. 3 The CV curves (a) of BDD electrodes with linear relationship between current density and square root of scanning rate of BDD electrodes (b), Nyquist diagram of BDD and Randles equivalent circuit (c), current density *vs.* time curve (d), oxygen evolution polarization curve (e) with and without 50 mg L^{-1} landfill leachate added to 0.1 M Na_2SO_4, oxygen evolution polarization curve (f) in 0.5 M H_2SO_4, oxygen evolution polarization curve (g) and linear relationship between current density and square root of scan rate in 0.1 M Na_2SO_4 containing 50 mg L^{-1} landfill leachate (h), and detection of hydroxyl free concentration with time (i).

leachate was added, the response current density of BDD electrode was 15.42 mA cm^{-2}. The addition of landfill leachate increases the response current density of the electrode, which is thought to be caused by the oxidation of the leachate. This further proves that BDD has greater potential for electrocatalytic degradation of late landfill leachate. Thereafter, the LSV curve of landfill leachate added with 50 mg L^{-1} was tested (Fig. 3g) to analyze its oxidation mechanism. As expected, no oxidation peak occurred before the oxygen evolution reaction due to the direct oxidation. The linear relationship between the peak current density and the square root of the scanning rate (Fig. 3h) indicates that the electrochemical oxidation of landfill leachate at the BDD electrode is controlled by mass transfer, where the diffusion of the filtrate from the primary solution to the electrode surface may be the limiting step. In order to verify the degradation rate of BDD electrode, N-subunit *N*-methyl-aniline was used to detect the concentration of ˙OH radical (Fig. 3i). Notably, it was found that the ˙OH radical concentration basically increased linearly with the increase of time, which was consistent with the literature reports,[44] ensuring the contribution of electrochemical degradation of late landfill leachate.

Moreover, the analysis of the influence factors and effect of BDD electrode on the electrochemical degradation of late landfill leachate is the key to evaluate the organic migration and transformation path of boron-doped diamond electrocatalytic degradation of landfill leachate. To explore the promising potential in electrocatalytic degradation of landfill leachate, the influence factors of current density, A/V, and pH values on the effect (COD, TOC, and UV$_{254}$ removal rate) of BDD electrode were investigated in Fig. 4.

Current density is an important factor affecting the removal of pollutants in the electrochemical oxidation process, and its selection usually depends on the concentration of pollutants and the expected treatment effect. Under the condition that A/V value is 4.25 m^{-1}, initial pH is not adjusted, plate spacing is 5 cm, and reaction time is 1 to 5 h, the effect of current densities (50, 70, 90) mA cm^{-2} on COD, UV$_{254}$ and TOC were evaluated in Fig. 4a–c. The COD removal rate of landfill leachate can be improved by increasing the current density. As shown in Fig. 4a, when the current density is 50 mA cm^{-2}, the COD removal rate is 76.85% after electrochemical oxidation for 5 h. When the current density continues to increase to 90 mA cm^{-2}, the COD removal rate can be increased to 97.27%. When the current density is constant, the degradation rate increases linearly with the increase of time and temperature, contributing to a stronger COD degradation rate. Meanwhile, the absorption rate of UV$_{254}$ increased significantly with the increase of reaction, and gradually becomes stable when the reaction time is greater than 4 h at different current densities in Fig. 4b. As the current density increased from 50 mA cm^{-2} to 90 mA cm^{-2}, the removal rate of UV$_{254}$ increased significantly from 58% to 98%. Moreover, TOC removal rate showed the same trend as COD and UV$_{254}$ results, increasing significantly with the increase of current density. When the current density increases from 50 mA cm^{-2} to 90 mA cm^{-2}, the TOC removal rate increases from 77% to 90%, and the further increase has no significant contribution to the TOC

removal rate Fig. 4c. Notably, the change trend of TOC concentration satisfies the exponential equation, indicating that TOC removal is mainly controlled by mass transfer process during electrochemical oxidation.

Apparently, the A/V values (3.4 m^{-1}, 4.25 m^{-1}, 5.67 m^{-1}) do have a certain influence on the removal of organic matter in the electrochemical oxidation of landfill leachate under current density of 90 mA cm^{-2} in Fig. 4d–f. The effects of A/V values on electrochemical oxidation of landfill leachate (COD, TOC, and UV$_{254}$ removal rate) by BDD electrode show a same trend as the analysis of current density. Typically, the influence of A/V value on COD, TOC and UV$_{254}$ may be attributed to the following reasons. When the current density is constant, the total amount of organic matter contained in landfill leachate will also decrease when the water quantity decreases, so the removal rate of organic matter per unit time will increase. When the water volume is small, the temperature of landfill leachate increases greatly due to the thermal effect of the current, which helps to strengthen the mass transfer process. Obviously, with the increase of current density, the effluent temperature after degradation of landfill leachate increases gradually in Fig. S3† Hence, the removal effect of COD, TOC and UV$_{254}$ is significantly enhanced with the increase of A/V value, especially the A/V value of 5.67 m^{-1}.

Furthermore, a slight difference of electrochemical oxidation of landfill leachate under the increased pH values was noticed as compared with current density and A/V values. As shown in Fig. 4g–i, as the initial pH decreased from 8.5 to 5.5, the COD removal rate showed a gradual upward trend from 90% to about 98%. This increase in acidic condition was mainly attributed to that a large amount of carbonates and bicarbonates are converted into CO$_2$, leading to a decrease in consuming hydroxyl radicals produced by electrochemical oxidation process. Hence, it is conducive to the removal of organic matter for improving the COD removal rate. Similarly, with the increase of initial pH, the removal rate of UV$_{254}$ decreased, indicating that acidic conditions were conducive to increasing the removal rate of UV$_{254}$. However, compared to acidic conditions, TOC removal was up to 93% at pH 8.5. It is suggested that alkaline condition is beneficial to improve TOC removal of late stage landfill leachate by electrochemical oxidation of BDD electrode. This may be due to the fact that the landfill leachate contains a lot of NH$_3$–N and carbonate, which has a strong buffering capacity. However, adjusting pH will consume a lot of chemicals, which will cause an increase in cost. So, comprehensive analysis shows that pH 8.5 can take into account both degradation effect and cost-effectiveness.

More importantly, mechanism of organic migration and transformation through electrocatalytic degradation of late landfill leachate by boron-doped diamond anode has still not been systematically studied. Three-dimensional fluorescence spectroscopy (EEM) and GC-MS spectra were adopted to study the migration and transformation of organic pollutants from late landfill leachate at different electrolysis time because of its high accuracy and sensitivity in characterizing pollutant types and structure information. As shown in Fig. 5a–d and Table S2,† the organic fluorescent substances contained in the landfill
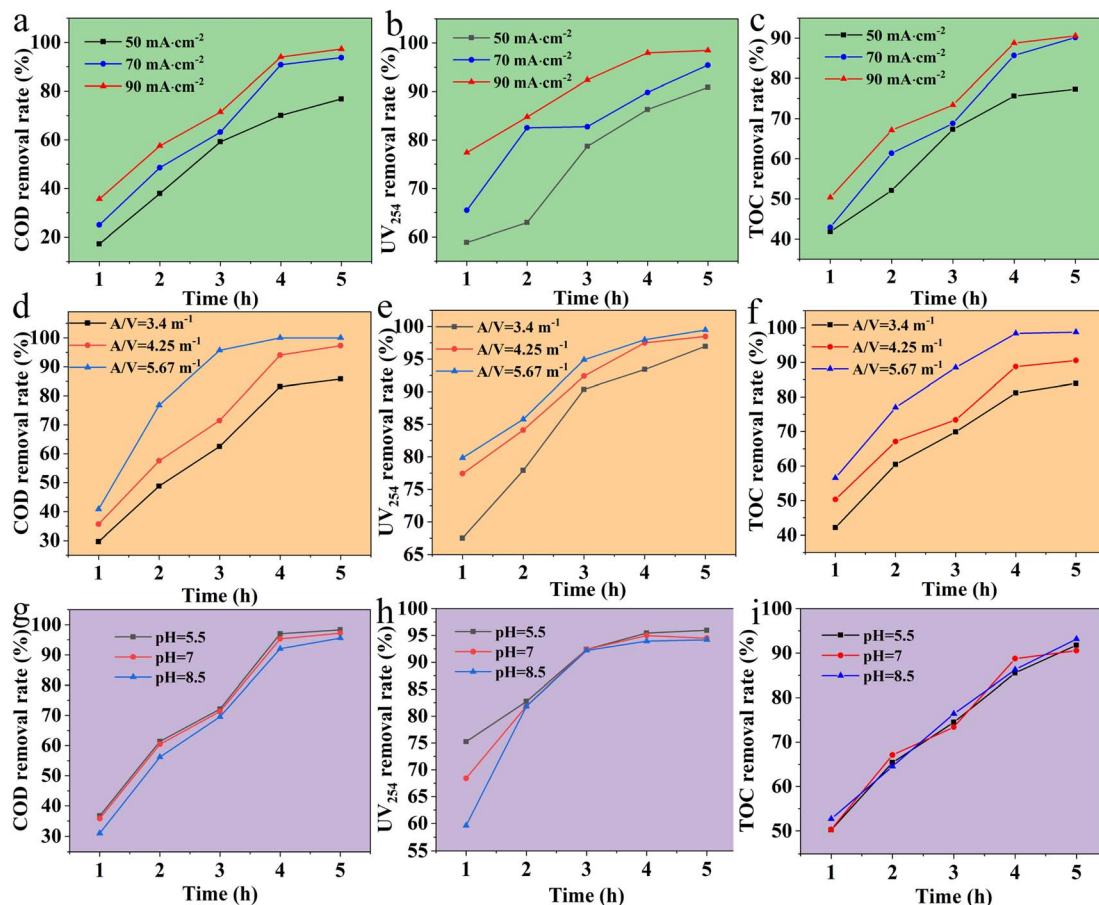
Fig. 4 The influence factors of current density (a–c), A/V values (d–f), pH values (g–i) on the effect (COD, TOC, and UV$_{254}$ removal rate) of BDD electrode on the electrochemical degradation of late landfill leachate.

leachate were mainly aromatic proteins, fulvic acids, humic acids and soluble biometabolites, among which fulvic acids accounted for a large proportion in the leachate. Indeed, with the extension of electrochemical degradation time, the concentrations and types of various organic fluorescent substances in landfill leachate changed in Fig. 5e. It indicates that the composition proportion of organic fluorescent substances in landfill leachate is constantly changing, and indirectly confirms that there are differences in the removal efficiency of organic compounds with different properties by electrochemical degradation. Concretely, after electrochemical degradation, the content of humic acid has significantly decreased. Although the proportion has changed, the overall content still decreases in Fig. S4.† And more, before the reaction, the percentage of fluorescence intensity of each region in the total fluorescence intensity was V, III, IV, II and I in descending order. When the reaction time is less than 4 h, the percentage content of several regions remains unchanged, while when the reaction time is 5 h, the percentage of the fluorescence intensity of each region in the total fluorescence intensity is III, IV, V, II, and I in descending order. The results showed that the degradation effect of humic acid by electrochemical oxidation was better than that of fulvic acid and soluble biometabolites.

Biodegradability (BOD$_5$/COD) is an important indicator for evaluating the difficulty of microbial degradation of pollutants in water. As shown in Fig. 5f, when the current density remains constant, the biodegradability of the effluent from the leachate treatment gradually increases with the prolongation of reaction time. When the current density is less than 90 mA cm^{-2}, the increase in biodegradability of the leachate decreases when the reaction time is > 3 h. The reason is that OH selectively oxidizes both biodegradable and non biodegradable organic compounds, resulting in a decrease in the content of biodegradable organic compounds. When the current density is 90 mA cm^{-2} at <3 h, the effluent from electrochemical oxidation of landfill leachate has the best biodegradability. When the A/V value increases, the biochemical properties significantly increase over time. The reason is that electrochemical oxidation makes it easier to biodegrade difficult organic compounds, increasing the proportion of biodegradable organic compounds in the total organic matter. The effects of different initial pH showed that alkaline conditions were beneficial to the degradation of landfill leachate by BDD electrode. This is because more hydroxyl radicals participate in the electrochemical oxidation process of organic matter under acidic conditions, and the selectivity of this process is low. Besides, a large amount of biodegradable organic matter will also be decomposed.
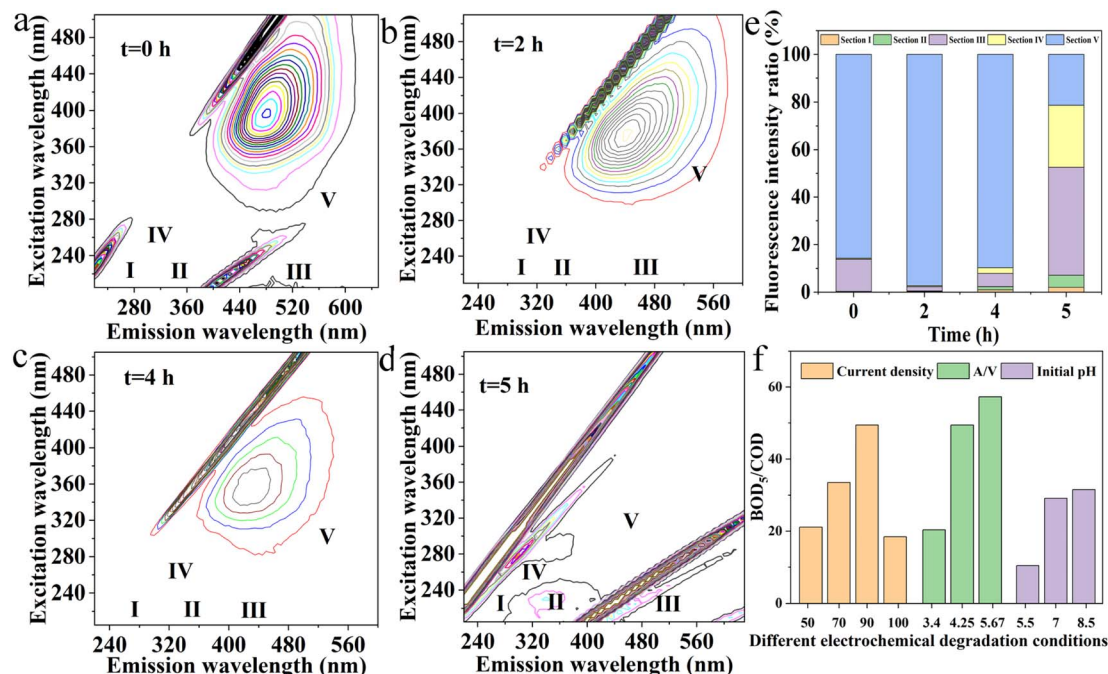
Fig. 5 The excitation-emission matrix spectroscopy (EEM) (a–d) of late landfill leachate at different electrolysis time testing condition: current density of 90 mA cm^{-2}, A/V value of 5.67 m^{-1}, pH of 5.67, the percentage of fluorescence intensity in different reaction times and regions to the total fluorescence intensity (e), comparison of biodegradability under different conditions (f).

Therefore, the biodegradability of leachate treatment effluent is lower than that of other pH values.

Simultaneously, the organic species from late landfill leachate at different electrolysis time were analyzed by GC-MS spectra. As can be seen from Fig. 6 and Table S3,† the organic composition of landfill leachate is very complex, and there are more than 60 distinct characteristic peaks on the GC-MS spectrum, with more organic compounds such as phenols, esters, amides and heterocycles occupying a large percentage.

As shown in Table S4,† with the extension of electrochemical degradation time, the types of organic matter decreased, and the amide/olefin and alcohol phenolic compounds were all degraded after 5 h of degradation, indicating that these two substances were transformed into other substances or decomposed into CO_2 and H_2O in the electrochemical oxidation process. In addition, the types and quantities of alkane organic substances gradually increased, especially the content of straight chain alkane increased significantly. This indicates that other macromolecular organic compounds (alcohols, phenols, etc.) are continuously decomposed into alkanes in the electrochemical oxidation process. But, the types and quantities of ester compounds first increase and then decrease, which may be due to the fact that there are more acidic substances in the stock solution, and the pH value decreases and ester substances are formed with the consumption of OH. Besides, organic compounds with a molecular weight less than 300 gradually decrease, indicating the gradual decomposition of alcohols and olefins; An increase in organic matter with a weight greater than 300 indicates that unsaturated organic matter is continuously decomposing into stable substance.

Followingly, migration and transformation of ammonia nitrogen during electrochemical oxidation was evaluated at different current densities, A/V, and pH values in Fig. 7a–c. When the current density is 50 mA cm^{-2} and the reaction time is less than 4 h, the ammonia nitrogen concentration is increased, and the removal rate of ammonia nitrogen reaches 50% after 5 h (Fig. S5†). When the current density is 70 mA cm^{-2} and the reaction time is less than 2 h, ammonia nitrogen concentration gradually decreases, and all ammonia nitrogen is removed at 5 h. When the current density is 90 mA cm^{-2}, the removal rate of ammonia nitrogen increases significantly from 1 to 5 h, and all ammonia nitrogen is removed at 5 h. The reason for the rise of ammonia nitrogen may be from the breaking of the high molecular weight nitrogenated compounds. When the current density is low, the ammonia nitrogen generation rate of ammonia nitrogen is greater than the removal rate of ammonia nitrogen. Therefore, when the current density is 50 mA cm^{-2} and 70 mA cm^{-2}, the removal rate of ammonia nitrogen is negative when the degradation time is less than 3 h (Fig. S5†). When the current density is 90 mA cm^{-2}, the removal rate of ammonia nitrogen is higher than the generation rate, showing a different trend from that under 50 mA cm^{-2} and 70 mA cm^{-2} (Fig. S5†). In order to verify this phenomenon, the removal efficiency of ammonia nitrogen can reach 30% for only 1 h at 100 mA cm^{-2} (Fig. S6†). The results show that increasing the current density can effectively reduce the proportion of ammonia nitrogen converted into chloramine. The decreases in ammonia nitrogen concentration was attributed to that the amount of active chlorine is gradually increased, which speeds up the reaction rate of chloramine conversion to nitrogen in the
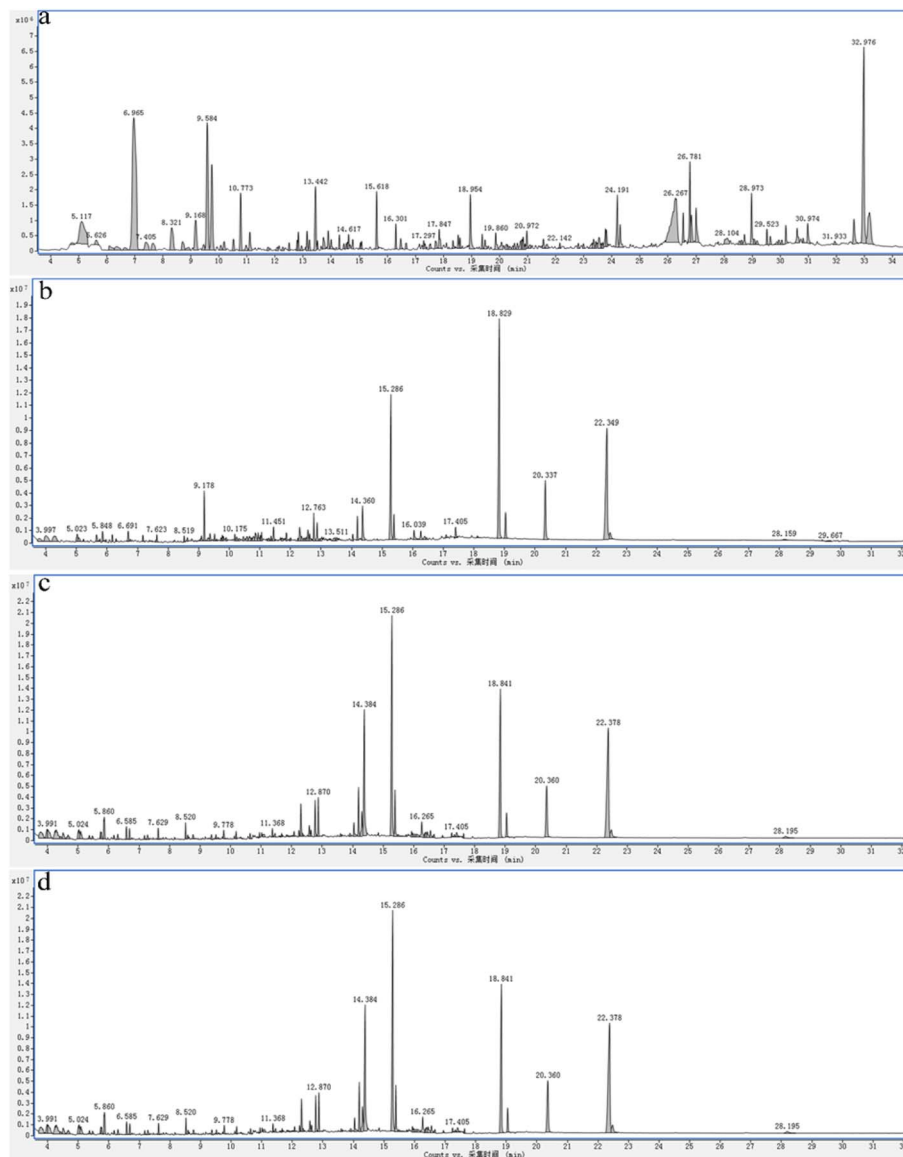
Paper

Fig. 6 GC-MS spectra of late landfill leachate degraded by BDD electrodes during oxidation at 0 h (a), 2 h (b), 4 h (c), and 5 h (d).

electrochemical oxidation process. In addition, as show in Fig. 7a, nitrate concentration increased significantly during nitrogen conversion. As shown in Fig. S7,† the rate and concentration of nitrate production increased significantly with the increase of current density, and the nitrate concentration was 206.68 mg L^{-1} at 90 mA cm^{-2}. For other nitrogen conversions, including nitrogen and chloramines, the content of other nitrogen decreases as the current density increases.

For the effect of A/V values on evolution of ammonia nitrogen, when the A/V value is 3.4 m^{-1} and the reaction time is 1 h, the ammonia nitrogen concentration increases, and the ammonia nitrogen removal rate increases significantly after 1 h; while when the A/V value is 4.25 m^{-1} and 5.67 m^{-1}, the ammonia nitrogen removal rate rises linearly, and the ammonia nitrogen is completely removed after 5 h of electrochemical oxidation (Fig. S8†). The reason for the short-term increase of

ammonia nitrogen concentration caused by low A/V value may be that the mass transfer is affected by low temperature, resulting in the formation rate greater than the consumption rate. However, with the increase of A/V value, the conversion rate of other nitrogen also increases gradually along with the linear decline of ammonia nitrogen concentration in Fig. 7b. When A/V value is 5.67 m^{-1}, the electrochemical oxidation for 4 h will remove all ammonia nitrogen, and the concentration of other nitrogen is also very low. When the A/V value is 4.25 m^{-1} and the electrochemical oxidation takes place for 4 h, all ammonia nitrogen is removed, and the concentration of other nitrogen is higher than that of other nitrogen with A/V of 5.67 m^{-1}, and there may be accumulation of chloramines in the intermediate process. As the A/V value increases, the concentration of nitrate increases linearly with reaction time, when all ammonia nitrogen is removed, the accumulation rate of nitrate
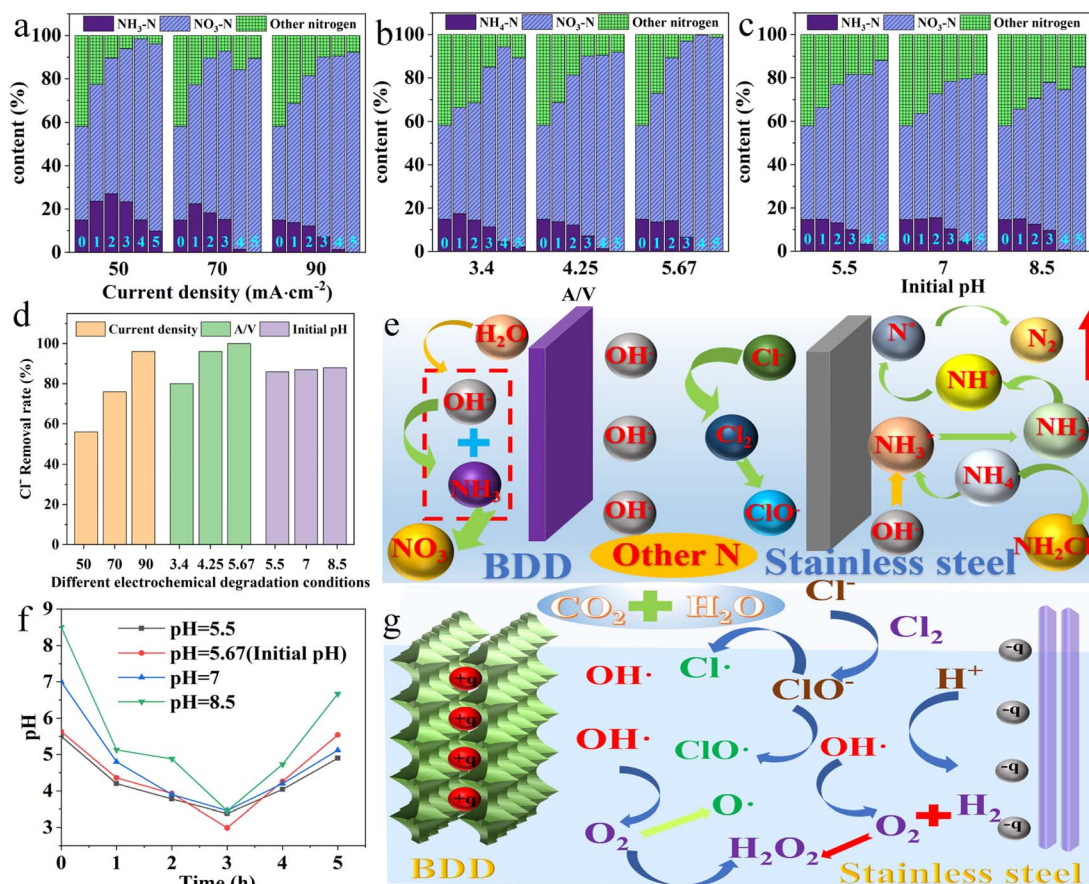
Fig. 7 The evolution of ammonia (a–c) and Cl⁻ removal rate (d) at different current density, A/V values, and pH values, schematic of ammonia nitrogen conversion pathway (e), pH change with time at different initial pH values (f), electrolysis mechanism on late landfill leachate by BDD electrode (g).

gradually decreases in Fig. S9.† For the effect of pH values on evolution of ammonia nitrogen, the removal rate of ammonia nitrogen increased significantly with the increase of pH values in Fig. S10.†

After 1 h of reaction, the concentration of ammonia nitrogen remained almost unchanged. This is because the initial pH has an impact on the change of active chlorine species during the electrochemical oxidation process. As time increased, the removal rate of ammonia nitrogen significantly increased. After 5 h of electrochemical oxidation, all ammonia nitrogen was removed. When pH = 8.5, the reaction time was less than 5 h, and the rate of ammonia nitrogen decrease was the fastest in Fig. S10.† This is because under alkaline conditions, NH_4^+ tends to convert to $NH_3 \cdot H_2O$, at this time, ammonia nitrogen in the solution mainly exists in the form of $NH_3 \cdot H_2O$, and the volatilization and escape of ammonia gas promote the removal of ammonia nitrogen in the solution. In addition, other nitrogen concentrations decrease with increasing pH in Fig. 7c, while nitrate concentration increases linearly. Fig. S11† show that nitrate concentration is the lowest at pH = 8.5, indicating that alkaline conditions help to reduce nitrate concentration.

As the landfill leachate contains a large number of active chloride ions, which cannot be fully utilized during the removal

of ammonia nitrogen, chloramines will also be produced during in the electrochemical oxidation process. So, the electrochemical oxidation method used as a pre-treatment unit, these chlorine-containing compounds may adversely affect the pollutant removal effect of subsequent biological treatment. As shown in Fig. 7d, the removal rate of chloride ions increased from 56% to 96% with the current density increasing from 50 mA cm⁻² to 90 mA cm⁻². When the current density is constant, the removal rate of chloride ions increases significantly with the increase of A/V value. It is worth mentioning that when the A/V value is 5.67 m⁻¹, chloride ions are completely removed. Through the five-step test, it is found that chloride in water mainly exists in ClO_3^-, with a small amount of chlorine gas. When the current density is 90 mA cm⁻², A/V value is 4.25 m⁻¹, and the initial pH value is adjusted to 5.5, 7 and 8.5, it can be seen that the chloride ion concentration decreases significantly with the increase of pH value. When pH is 8.5, the chloride ion removal rate is the highest. By detecting the chloride, the concentrations of ClO_3^- and ClO_2^- increase significantly. The measure of electrical conductivity show that the rate of decrease of electrical conductivity is slow, which indicates the existence of free chlorine in water on the other hand. It also further shows that the production of active chlorine is conducive to the

Paper

degradation of pollutants (Table S5†). Fig. S12† show that the slow decrease in conductivity indicates the presence of free chlorine in the water. The production of active chlorine is beneficial for the degradation of organic matter. The magnitude of conductivity is directly proportional to the salt content in water, and its decrease also indicates that organic matter is constantly degrading with large molecules breaking down into small molecules and continuously combining with ions in water, ultimately becoming CO_2 and H_2O.

Apart from migration and transformation of ammonia nitrogen and chloramines, the relationship between the initial pH change of landfill leachate and the pH change of effluent after electrochemical oxidation is crucial and indispensable for the analysis of the mechanism of electrochemical oxidation, recorded in Fig. 7e and f. Remarkably, with the increase of time, the pH value first decreases and then rises. The pH value drops to the lowest point at 3 h and then gradually rises. The reason is that with the increase of oxidation time, the pH value decreases due to the continuous consumption of OH^-, but when the ammonia nitrogen is exhausted, the continuous accumulation of OH^- leads to the rise of pH values. Also, the consumption of the organic acid formed during the degradation of the organic compounds. Given the ability to degrade BDD, the energy consumption of the proposed system also has been determined. As shown in Fig. S13,† the increase in current densities and A/V values leads to an increase in energy consumption, while pH changes have little effect on variable in energy consumption. Overall, this relatively high energy consumption may be due to the large spacing between electrodes, high current density, and high A/V value.

Overall, the BDD electrode is a typical inactive electrode, and the reactive oxygen species formed on its surface belongs to the physically adsorbent "reactive oxygen species" (Fig. 7g). That is, OH^- is only physically adsorbed on the electrode surface and will not bind to the active site on the electrode surface. Obviously, no selectivity in oxidizing organic matter, $OH^•$ has a good oxidative degradation effect on most organic compounds in late landfill leachate. Moreover, in addition to hydroxyl radicals, organics may also be oxidized by active chlorine (Cl_2, $HClO$, ClO^-), $C_2O_6^{2-}$, $S_2O_8^{2-}$, $P_2O_8^{2-}$ and other reactive oxygen species ($O^•$, $HO_2^•$, O_3, H_2O_2).

4 Conclusion

In summary, the effect of BDD anode on the removal of pollutants from late landfill leachate was studied by electrochemical oxidation. Detailedly, the influence of factors on the removal of organic matter and ammonia nitrogen in the electrochemical oxidation process was analyzed to obtain the optimized conditions for improving the biodegradability of late stage leachate. Increasing the current density and A/V value can improve the removal effect of organic matter and ammonia nitrogen. When the current density is 90 mA cm^{-2}, pH is 8.5, plate spacing is 5 cm, and A/V value is 5.67 m^{-1}, the removal rates of TOC and NH_3–N after electrochemical oxidation for 5 h can reach 99% and 100%, respectively. Alkaline conditions not only help to improve the removal rate of TOC and ammonia

nitrogen, but also play a positive role in reducing the concentration of nitrate. More importantly, EEM and GC-MS showed that BDD electrode could effectively degrade organic matter in landfill leachate, and the types of organic matter decreased with the increase of time, in which amides and olefin substances were all degraded, and ester substances decreased. Therefore, this study affords the comprehensive analysis of electrocatalytic degradation of late landfill leachate by boron-doped diamond anode for the mechanism of organic migration and transformation, which is significant for practical application.

Author contributions

The manuscript was written through contributions of all authors. All authors have given approval to the final version of the manuscript.

Conflicts of interest

The authors have no conflict of interest to declare.

Acknowledgements

References

1 P. Wijekoon, P. A. Koliyabandara, A. T. Cooray, S. S. Lam, B. C. Athapattu and M. Vithanage, *J. Hazard. Mater.*, 2022, **421**, 126627.
2 S. Ma, C. Zhou, J. Pan, G. Yang, C. Sun, Y. Liu, X. Chen and Z. Zhao, *J. Cleaner Prod.*, 2022, **333**, 130234.
3 C. Teng, K. Zhou, C. Peng and W. Chen, *Water Res.*, 2021, **203**, 117525.
4 A. Kamal, A. Makhatova, B. Yergali, A. Baidullayeva, A. Satayeva, J. Kim, V. J. Inglezakis and S. G. E. Poulopoulos, *Sustainability*, 2022, **14**(21), 14427.
5 P. Ashcheulov, A. Otake, A. Akai, A. Taylor, L. Klimša, P. Hubík, J. More-Chevalier and Y. Einaga, *Chem. Eng. J.*, 2023, **473**, 145463.
6 C. Wu, W. Chen, Z. Gu and Q. Li, *Sci. Total Environ.*, 2021, **762**, 143131.
7 S. Shi, D. Zhou, Y. Jiang, F. Cheng, J. Sun, Q. Guo, Y. Luo, Y. Chen and W. Liu, *Adv. Funct. Mater.*, 2024, 2312664.
8 S. Shi, Y. Jiang, H. Ren, S. Deng, J. Sun, F. Cheng, J. Jing and Y. Chen, *Nano-Micro Lett.*, 2024, **16**(1), 1–15.
9 L. Yang, Y. Heng, J. Sun, D. Hu and F. Cheng, *J. Cleaner Prod.*, 2024, 141964.
10 E. R. Bandala, A. Liu, B. Wijesiri, A. B. Zeidman and A. Goonetilleke, *Environ. Pollut.*, 2021, **291**, 118133.
11 D. Yu, J. Cui, X. Li, H. Zhang and Y. Pei, *Chemosphere*, 2020, **243**, 125438.
12 O. T. Can, L. Gazigil and R. Keyikoglu, *Environ. Prog. Sustainable Energy*, 2022, **41**(1), e13722.

13 Z. Tong, Z. Xi, W. Chen, X. Zhu, Y. Liu and C. Kang, *Fresenius Environ. Bull.*, 2022, 11388.

14 Y. Zhang, Z. Chen, P. Wu, Y. Duan, L. Zhou, Y. Lai, F. Wang and S. Li, *J. Hazard. Mater.*, 2020, **393**, 120448.

15 J. Tang, C. Su and Z. Shao, *Exploration*, 2024, **4**(1), 20220112.

16 Q. Yu, Y. Zhang, M. Tang, G. Liu and L. Li, *J. Water Proc. engineering*, 2023, **53**, 103603.

17 M. Y. Kilic, T. Yonar and B. K. Mert, *Clean – Soil Air Water*, 2014, **42**(5), 586–593.

18 T. Ren, X. Zhang, S. Chen, X. Huang and X. Zhang, *Sci. Total Environ.*, 2022, **843**, 156904.

19 D. Fang, J. Wang, D. Cui, X. Dong, C. Tang, L. Zhang and D. Yue, *J. Indian Inst. Sci.*, 2021, 1–40.

20 S. Park, E. T. Yun, H. J. Shin, J. Choi, J. Lee and D. W. Kim, *J. Water Proc. engineering*, 2023, **53**, 103670.

21 H. Li, J. Qin, M. Li, C. Li, S. Xu, L. Qian and B. Yang, *Sens. Actuators, B*, 2020, **302**, 127209.

22 X. You, X. Hu, Q. Sun, H. Wang, H. Wang and X. Hou, *Int. J. Miner., Metall. Mater.*, 2021, **28**, 1413–1428.

23 W. Yang, Z. Deng, Y. Wang, L. Ma, K. Zhou, L. Liu and Q. Wei, *Sep. Purif. Technol.*, 2022, **293**, 121100.

24 H. Wang, S. Zhou, T. Wang, Z. Zhou, Y. Huang, S. Handschuh-Wang, H. Li, Y. Zhao and Y. Tang, *J. Colloid Interface Sci.*, 2023, **652**, 1512–1521.

25 Y. Tang, M. Liu, D. He, R. Pan, W. Dong, S. Feng and L. Ma, *Chemosphere*, 2022, **307**, 135912.

26 J. Song, Y. Yinhai, Y. Jia, T. Wang, J. Wei, M. Wang, S. Zhou, Z. Li, Y. Hou, L. Lei and B. Yang, *Sep. Purif. Technol.*, 2021, **276**, 119350.

27 Y. Zhao and X. Zhao, *Int. J. Electrochem. Sci.*, 2021, **16**(4), 210441.

28 S.-J. Zhang, Y.-Z. Peng, S.-Y. Wang, S.-W. Zheng and J. Guo, *J. Environ. Sci.*, 2007, **19**(6), 647–651.

29 Y. Lei, J. Hou, C. Fang, Y. Tian, R. Naidu, J. Zhang, X. Zhang, Z. Zeng, Z. Cheng, J. He and D. Tian, *Ecotoxicol. Environ. Saf.*, 2023, **263**, 115366.

30 D. Yu, Y. Pei, Z. Ji, X. He and Z. Yao, *Chemosphere*, 2022, **291**, 132895.

31 L. Pisharody, A. Gopinath, M. Malhotra, P. V. Nidheesh and M. S. Kumar, *Chemosphere*, 2022, **287**, 132216.

32 Y. Einaga, *Acc. Chem. Res.*, 2022, **55**(24), 3605–3615.

33 P. Chen, Y. Mu, Y. Chen, L. Tian, X. H. Jiang, J. P. Zou and S. L. Luo, *Chemosphere*, 2022, **29**, 132817.

34 Y. Li, F. Tang, D. Xu and B. Xie, *Sustainability*, 2021, **13**(11), 6236.

35 Z. Liu, H. Li, M. Li, C. Li, L. Qian, L. Su and B. Yang, *Electrochim. Acta*, 2018, **290**, 109–117.

36 M. Ghazouani, H. Akrout and L. Bousselmi, *Environ. Sci. Pollut. Control Ser.*, 2017, **24**(11), 9895–9906.

37 R. Bogdanowicz, A. Fabiańska, L. Golunski, M. Sobaszek, M. Gnyba, J. Ryl and E. M. Diam, *Relat. Mater.*, 2013, **39**, 82–88.

38 W. Yang, J. Tan, Y. Chen, Z. Li, F. Liu, H. Long and Z. Yu, *J. Alloys Compd.*, 2022, **890**, 161760.

39 F. Zhang, Z. Song, J. Li, G. Chen, X. Jiang and Q. Cong, *Thin solid films*, 1991, **199**(1), 123–128.

40 X. Gao, W. Li, R. Mei, C. Zhu, B. Zhou, L. Ma and T. Liu, *J. Electroanal. Chem.*, 2019, **832**, 247–253.

41 K. Ushizawa, G. Mikka N, K. Watanabe, I. Sakaguchi, Y. Sato and T. Ando, *J. Raman Spectrosc.*, 1999, **30**(10), 957–961.

42 M. Pierpaoli, P. Jakobczyk, M. Sawczak, A. Łuczkiewicz, S. Fudala-Książek and R. Bogdanowicz, *J. Hazard. Mater.*, 2021, **401**, 123407.

43 S. Chai, Y. Wang, Y. N. Zhang, M. Liu, Y. Wang and G. Zhao, *Environ. Sci. Technol.*, 2017, **51**(14), 8067–8076.

44 C. Comninellis, *Electrochim. Acta*, 1994, **39**(11–12), 1857–1862.